

Turbulent flow over an axisymmetric body with annular cavity

I E Ivanov^{2,3}, I A Kryukov^{1,3}, E V Larina,³ and G S Glushko¹

¹ A. Ishlinsky Institute for Problems in Mechanics of the Russian Academy of Sciences, Vernadsky Prospect 101(1), Moscow, 119526, Russia

² Lomonosov Moscow State University, Moscow, 119991, Russia

³ Moscow Aviation Institute (National Research University), Moscow, 121993, Russia

E-mail: kryukov@ipmnet.ru

Abstract. The paper concerns the numerical simulation of turbulent flow over axisymmetric body with an annular cavity. The influence of the ratio of the length to the cavity depth on the flow structure in the cavity was numerically studied in the case of supersonic flow. The open or closed type of the flow was obtained depending on the ratio of the length to the cavity depth. Comparison with experimental data [9, 10, 13] shows a good agreement between calculated and experimental results. The phenomenon of gas dynamic hysteresis for the implementation of the open - closed flow type studied experimentally in [10] was numerically reproduced. Also it has been shown that experimental conditions [13] also may cause this type of hysteresis.

1. Introduction

The practical interest in a flow over an axisymmetric body with an annular cavity is caused by a rather wide use of such constructions in aerospace applications. Just as in a rectangular cavity there can be two types of flows depending on the ratio of the annular cavity length to the depth of that: an open flow type (in a short cavity) or a closed flow type (in a long cavity). In the first case a single annular recirculating flow emerges in the cavity, in the second case two separate flows appear in the opposite corners of the cavity. The intermediary state between these two types, where flow may also switch from one to the other, is termed as transitional. In addition the type of cavity flow is affected by the Mach number, the Reynolds number and the nature and state of the approach boundary layer. Many researchers pay extra attention to the possible gas dynamic hysteresis in the flow over cavities related to the reorganization of the separated flow regime. For example, the gas dynamic “open-closed” type hysteresis was experimentally found in the supersonic flow over an axisymmetric body with an annular rectangular cutout on a cylindrical surface [9, 10]. A supersonic flow over an axisymmetric body and the emergence of open and closed cavity flows were experimentally and numerically analyzed in [13, 14]. For comparison some results of numerical simulations for plane and three-dimensional cavity flows can be found in [7] and some experimental results can be found in [8].

2. Mathematical model and numerical method

The unsteady axisymmetric RANS set of equations closed by the two-equations k - ε turbulence model is used as a mathematical model. The version of the k - ε turbulence model used in this article was constructed in [3, 4] and reveals the influence of the non-equilibrium between the generation and



dissipation of turbulence and compressibility. This model was tested for a variety of supersonic flows and showed rather satisfactory results [5, 6].

The method described in [1, 2] was used for numerical solving the set of equations mentioned above. A high-resolution Godunov-type scheme based on MUSCL variable reconstruction and slope limiters was used as a basic scheme for approximating the inviscid part of the set of equations. The viscous terms of the set of equations were approximated by an unstructured grid analogue of the central difference method; all source terms were approximated by the explicit-implicit method [1]. The no-slip conditions were specified on the wall, the symmetry conditions were specified in the symmetry line and the non-reflective boundary conditions were specified on the free boundaries.

3. Numerical Simulation of Guvernyuk et al experiment [9, 10]

A supersonic flow with $M=3$ at zero angle of attack on an axisymmetric body which consists of a sharp cone and a cylinder with an annular cavity was numerically simulated following the experiment described in [9, 10]. The annular cavity has a rectangular section as shown in figure 1. The cone semi-apex angle $\beta=20^\circ$, distance between the cone body and the cavity $l=30$ mm and the cylinder diameter $D=45$ mm and depth of the cavity $h=8$ mm are all fixed. The cavity "floor" cylinder diameter can be evaluated as $d=D-2h=29$ mm. The relative cavity length $s=L/h$ may be varied within the $10 < s < 15$ range due to the L variation ($80 \text{ mm} < L < 120 \text{ mm}$).

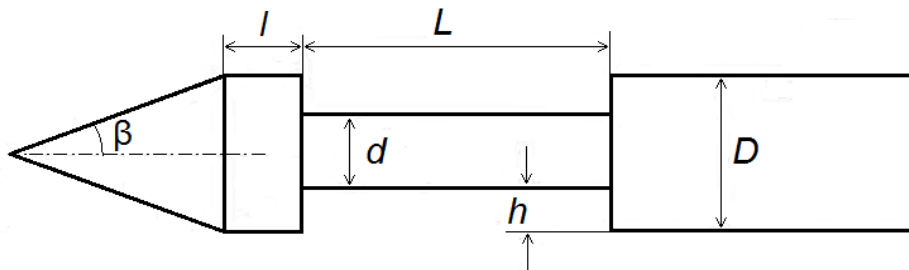


Figure 1. An axisymmetric body with an annular cavity [9, 10]

The computational mesh contains 400×150 cells for regular calculations and 800×300 cells for more accurate ones. The cavity is filled with 160×30 and 320×60 cells respectively.

In numerical calculations presented here as in the experiments [9, 10], the open-flow type was always obtained for small relative cavity length values $s < 10$. In this case the flow detaches from the cavity front lip and reattaches to the right vertical cavity wall near the rear edge. A recirculating flow consisted of one large and possibly several small vortexes in the corner regions with a subsonic flow regime is inside the cavity. The recirculating flow region is separated from the external flow by a mixing layer.

A supersonic ($M=3$) turbulent ($Re_\infty=1.7 \times 10^6$) flow over the axisymmetric body with the cavity was calculated for the relative cavity length range of $s=10 \div 16.25$ or for the cavity length range of $L=80 \div 130$ mm (see figure 1). The incident flow parameters are $P_\infty=16770$ Pa and $T_\infty=96.43^\circ\text{K}$. Figures from 2 to 4 show calculated results for $L=81$ mm ($s=10.125$).

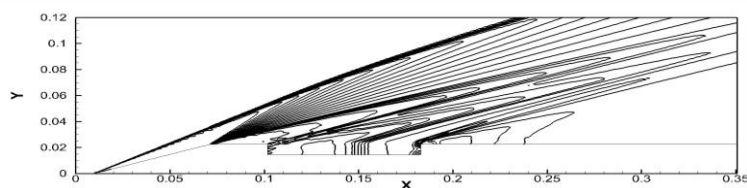


Figure 2. Pressure contour lines for $L=81$ mm.

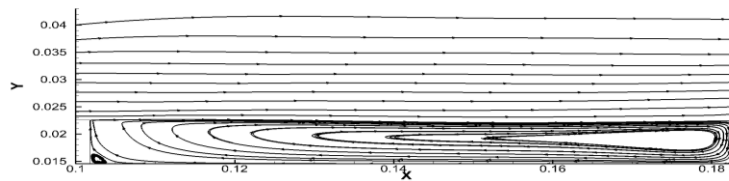


Figure 3. Streamlines inside the cavity for $L = 81$ mm.

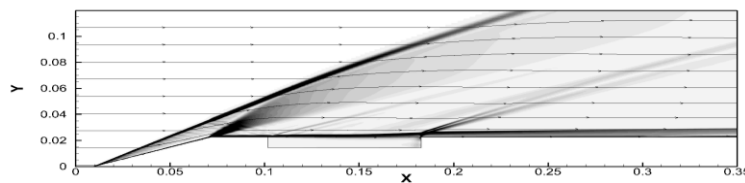


Figure 4. Density gradient and streamlines for $L = 81$ mm.

Figure 2 shows the pressure contour lines for $L = 81$ mm. Whole computational region has a size 0.4×0.2 m. Therefore most of the computational region is shown in the figure. Streamlines inside the cavity and in some vicinity of cavity are shown on figure 3. Figure 4 contains the numerical schlieren image (density gradient contours) and streamlines. From these figures the open-flow type with one large vortex and one small vortex in the forward corner can be easily seen.

When the relative cavity length exceeds a certain critical value $s > s_2$, there is the closed-flow type in the cavity. A closed type flow is characterized by a presence of two non-interacting or weakly interacting recirculating zones; the first recirculating zone is behind the front face of the cavity and the other zone is in vicinity of the rear face. The zones are separated by the external flow along the bottom of the cavity. The external flow is characterized by presence of strong shock waves and expansion waves caused by supersonic flow over the corner recirculating zones.

The flow over the body with annular cavity was calculated for the cavity length $L = 110$ mm ($s = 13.75$). The results are shown in figures 5–7.

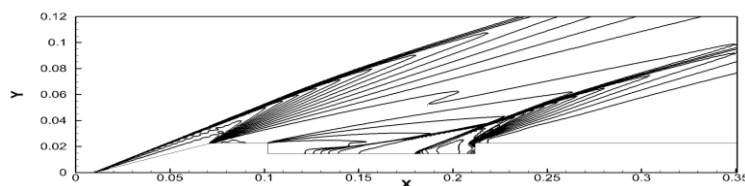


Figure 5. Pressure contour lines for $L = 110$ mm.

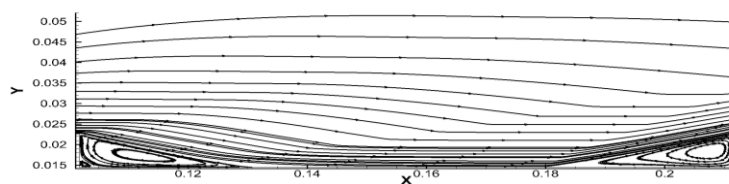


Figure 6. Streamlines inside the cavity for $L = 110$ mm.

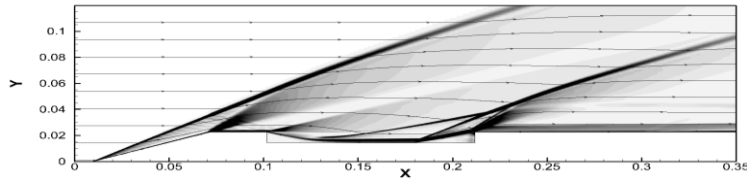


Figure 7. Density gradient and streamlines for $L = 110$ mm.

Figure 5 shows the pressure contour lines for $L=110$ mm. Streamlines inside the cavity and in some vicinity of cavity are shown in figure 5. Figure 7 contains the numerical schlieren image (density gradient contours) and streamlines. In these figures the closed-flow type with two vortices in the opposite corners of the cavity can be easily seen.

As mentioned before, the open-flow cavity type is realized for small relative cavity length values, while the flow inside the cavity formed by several vortices is separated from the external flow by a shear layer that spans the cavity and reattaches onto the rear face at or near the top corner (see figures 3 and 8a). The shear layer is curved towards the external flow. As s increases the mixing layer bends towards the cavity bottom while the vortex flow inside the cavity undergoes deformation: the main vortex looks to take shape of a butterfly, and the external flow gets closer to the cavity bottom (see figures 6 and 8b).

As a result of numerical simulation the critical values of the relative cavity length ($s_1=10.2$ ($L=81.5$ mm) and $s_2=13.8$ ($L=110.5$ mm)) when the flow structure changes from the open to the close type and vice versa were evaluated. Between the s_1 and s_2 values the flow type can be either open or closed depending on the flow development history.

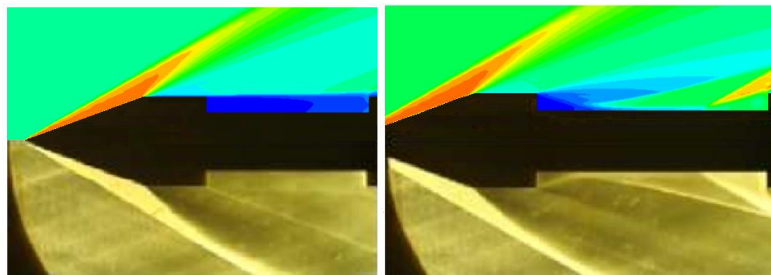


Figure 8. Comparison between numerical (top) and experimental schlieren (bottom) for $L=81$ mm (left) and $L=110$ mm (right).

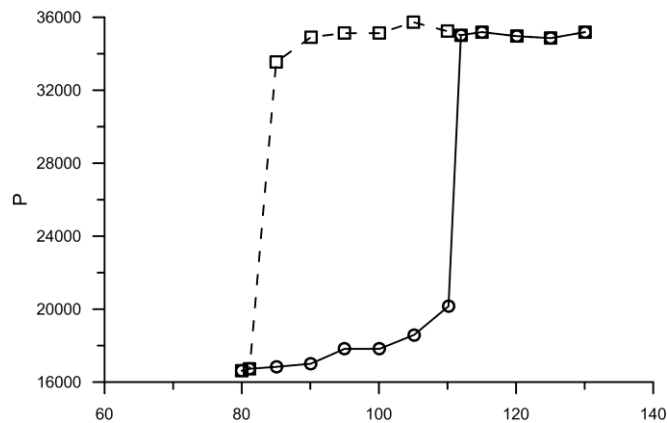


Figure 9. Dependence pressure P on the cavity length L in the rear corner of the cavity.

The presence of a gas dynamic hysteresis is illustrated in figure 9 by a dependence of the pressure, measured near the rear cavity corner, on the cavity length. The solid curve was obtained at an increasing s and the flow type changes from open to closed. The dashed curve was obtained at a decreasing s ; in this case the flow type changes from closed to open. Thus, the gas dynamic "open-closed" type hysteresis in the supersonic flow over an axisymmetric body with a rectangular annular cutout on the side surface of a cylindrical part of the body forms while the cutout length changes.

These results satisfactorily (accurate to 0.5 mm by transition points) match the experimental results from [10].

4. Numerical simulation of Mohri and Hillier experiment [13]

In this case the supersonic flow ($M=2.2$ at a zero angle of attack) over an axisymmetric body consisting of a sharp cone and a cylinder with a annular cutout was numerically simulated. The difference between this case and the previous one is in the fact that here the cavity starts right after the cone. Compare figures 1 and 10.

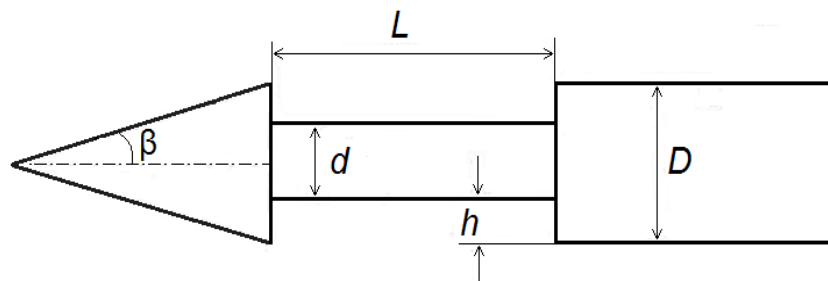


Figure 10. An axisymmetric body with an annular cavity [13].

The semi-apex angle is $\beta=16^\circ$, the cavity begins just behind the cone, the cavity 'floor' cylinder diameter is $d=9$ mm, the cylinder diameter is $D=15$ mm, the cavity depth is $h=3$ mm, $D=d+2h$. The relative cavity length $s=L/h$ varies in the $1.67 < s < 14.33$ range due to the L variation ($3 \text{ mm} < L < 41 \text{ mm}$). The incident flow parameters are $P_\infty=25250$ Pa, $T_\infty=146.34^\circ\text{K}$, $\text{Re}_\infty=0.87 \times 10^6$.

Figures from 11 to 13 show calculated results for $L=37$ mm ($s=12.33$). These figures show the pressure contour lines, streamlines inside the cavity and the numerical schlieren image (density gradient contours). It can be seen in figure 12, the flow in the cavity at $L=37$ mm has two recirculating zones, the first one is formed by the boundary layer separating from the front cavity lip and reattaching to the cavity 'floor' (the flow behind the backward step). The second recirculating zone is located between the separation point of the boundary layer from the cavity 'floor' and the reattachment point on the cavity back face (the flow over the forward step). These two recirculating zones are separated by the external flow along the cavity 'floor' and don't noticeably influence one another at large cavity length L values.

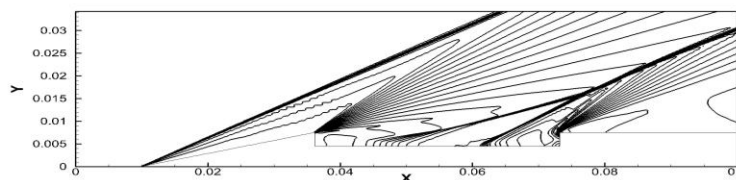


Figure 11. Pressure contour lines for $L=37$ mm.

For comparison the numerical density contours (upper part of figure) and experimental schlieren image (bottom part of figure) are shown together in a single scale in figure 14. A good agreement in shape and position of all main discontinuities in the flow can be seen.

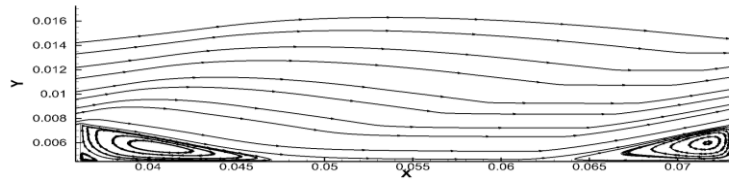


Figure 12. Streamlines inside the cavity for $L = 37$ mm.

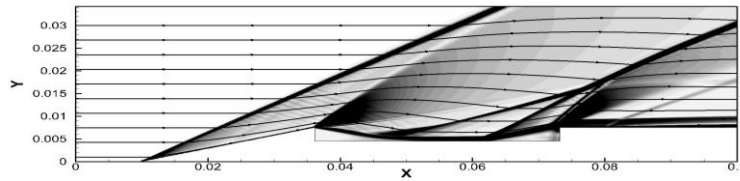


Figure 13. Density gradient and streamlines for $L = 37$ mm.

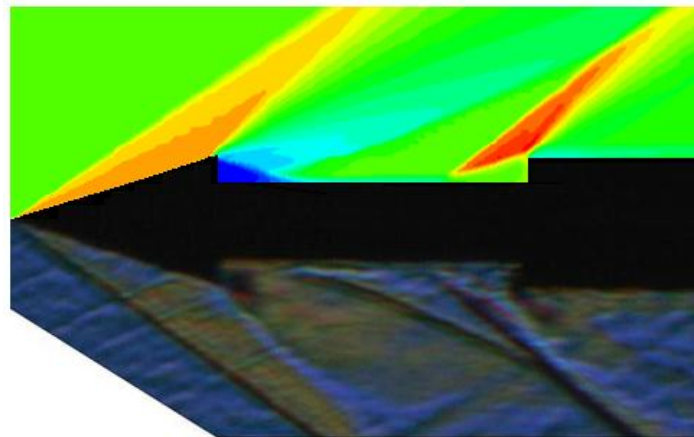


Figure 14. Comparison between CFD density distribution (top) and experimental schlieren [13] (bottom) for $L = 37$ mm.

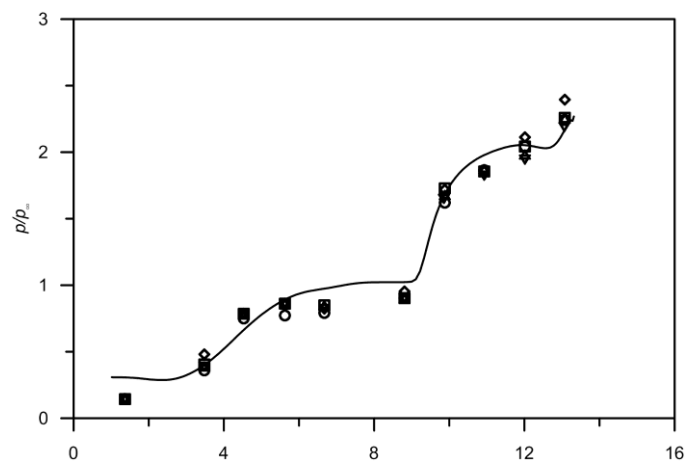


Figure 15. Experimental [13] and computational surface pressure distribution on the cavity floor for $L = 37$ mm.

5. Analysis of calculated results and comparison with the experiment

The comparison of calculated and experimental data in figures 14 and 15 shows that the results are matching well in flow structure (see figure 14), in detached zone length, in shock waves' and expansion fans' position. Also the local flow parameters are matching satisfactorily in relative pressure distribution on the cavity floor. The points of flow attachment and separation from the cavity bottom were predicted rather well by the location of pressure increase areas. The pressure level in the external flow near the cavity bottom is 5÷8% higher in the simulation than in the experiment. The largest pressure level difference is registered in the separation zone behind the forward lip of cavity at a maximum 3 mm distance behind the cone: in that area the measured relative pressure is $P/P_\infty < 0.2$, compared to the calculated $P/P_\infty = 0.28 \div 0.3$. This difference can be explained by the following way: in the experiment, as stated in [13], the flow over the conical fore-body of the axisymmetric body is laminar; a tripping disk was inserted behind the cone for flow turbulization. The disk adjoined directly on the front corner of the cavity and had a diameter slightly bigger than the diameter D . As a result a turbulent flow mode with a corresponding flow structure (figure 14) was set in the cavity. In the numerical simulation due to the $k-\varepsilon$ model peculiarities the laminar-turbulent transition happens very closely to the conical fore-body apex and thus the flow over almost the whole conical fore-body is turbulent. The difference in the flow mode in calculation and experiment and also in the turbulence parameters in the cavity can lead to different levels of calculated and experimental pressure in the front separation zone (base pressure).

Experimental and calculated data on supersonic flow over sharp cones was processed and published in the book [11] (in the chapter "Base pressure behind the backward step"). The dependence of base pressure on the Mach number in an incident flow was determined. The relative base pressure takes values $P/P_\infty = 0.31 \div 0.46$ for air flow $M=2.2$ over a cone with a semi-apex angle of 15° , which slightly exceeds the pressure behind the front face of the cavity in this article's calculation and is a considerably higher than the pressure measured in experiment [13].

The ratio of the mean base pressure to the pressure in the incident flow in the case of a flow with a Mach number $M=2.2$ and an isentropic index γ is described well by a semi-empirical formula

$$p_b = 0.15 + \left(1 + \frac{\gamma - 1}{2} M^2 \right)^{-(\gamma + 1)/\gamma}$$

obtained at the Khristianovich Institute of Theoretical and Applied Mechanics (Siberian branch of Russian Academy of Sciences) [12] based on a lot of experimental data in the Mach number range 1.5÷14 [15]. In the case of our calculation for $M=2.2$ and $\gamma=1.4$ this formula gives an estimation of base pressure $P/P_\infty = 0.46$, which corresponds to the value shown in [11] at this Mach number.

As a result of the numerical research a gas dynamic "open-closed" flow type hysteresis was also found for the experimental conditions. The hysteresis is close to [9; 10] with critical parameters of relative cavity length $s_1=10.5$ and $s_2=12.75$. In [13] the gas dynamic hysteresis was not studied experimentally.

6. Conclusion

The supersonic flow over an axisymmetric body with an angular cavity is studied numerically. Two physical experiments for incidental flow Mach numbers $M=3.0$ and $M=2.2$ are numerically simulated. The flow has either of an open or of closed type depending on relative cavity length. The hysteresis phenomenon was numerically reproduced for various flow types (open and closed) for both experiments.

Acknowledgement

The work was performed within the framework of the Program of basic research of the Russian academy of sciences and was funded by RFBR grants №16-01-00444a, №16-38-60185, №14-08-01286.

References

- [1] Glushko G S, Ivanov I E and Kryukov I A 2010 *Math. Models Comput. Simul.* **2** 407-22
- [2] Ivanov I E and Kryukov I A 1996 *Matematicheskoe Modelirovanie* **8** 6 47–55
- [3] Kryukov I A 2009 *Vestnik of Moscow Aviation Institute* **16** 2 101-8
- [4] Glushko G S, Ivanov I E and Kryukov I A 2010 Turbulence modeling for supersonic jet flows *Physical-Chemical Kinetics in Gas Dynamics* **9** <http://chemphys.edu.ru/issues/2010-9/articles/142/>
- [5] Ivanov I E, Kryukov I A and Larina E V 2013 Numerical simulation of shock wave turbulent boundary layer interaction for compression corner flow *Physical-Chemical Kinetics in Gas Dynamics* **14** <http://chemphys.edu.ru/issues/2013-14-4/articles/424/>
- [6] Ivanov I E, Kryukov I A and Larina E V 2014 Numerical simulation of high-speed viscous intake flow *Physical-Chemical Kinetics in Gas Dynamics* **15** <http://chemphys.edu.ru/issues/2014-15-4/articles/240/>
- [7] Lawson S J and Barakos G N 2011 *Progress in Aerospace Sciences* **47** 186–216
- [8] Kotov M A, Ruleva L B, Solodovnikov S I and Surzhikov S T 2014 Investigation of shock wave process of model flow in hypersonic aerodynamic shock tube // *Physical-Chemical Kinetics in Gas Dynamics* **15** <http://chemphys.edu.ru/issues/2014-15-3/articles/223/>
- [9] Guvernyuk S V, Zubkov A F, Simonenko M M, and Shvetz A I 2014 *Fluid Dynamics* **49** 540–6.
- [10] Guvernyuk S V, Zubkov A F and Simonenko M M 2014 On the observation of the aerodynamic hysteresis in supersonic flow over a ring cavity on an axisymmetric body *Advances in the Mechanics of Continuous Media, Collected papers at the Int. Conf. timed to the 75th birthday of Academician V. A. Levin* (Irkutsk : Megaprint) pp 163–8
- [11] Lavruhin G N and Popovich K F 2009 *Ajerogazodinamika Reaktivnyh Sopel* vol 2 (Moscow: FIZMATLIT) p 312
- [12] Zubkov A I, Garanin A F, Safronov V F, Sukhanovskaya L D and Tretyakov P K 2005 Supersonic flow past an axisymmetric body with combustion in separation zones at the body nose and base *Thermophysics and Aeromechanics* **12** 1-12
- [13] Mohri K and Hillier R 2011 *Shock Waves* **21** 175-91
- [14] Sinha J 2013 *Advances in Aerospace Science and Applications* **3** 83-90
- [15] Lutsky A E, Menshov A S and Khankhasaeva Y V 2014 The use of free boundary method for solving the problem of the flow past moving bodies KIAM Preprint № 93